Temperature and Phase Effects on the Overtone Spectra of Several Adamantanes

Daryl L. Howard and Bryan R. Henry*

Department of Chemistry and Biochemistry, University of Guelph, Guelph, Ontario, N1G 2W1, Canada

Received: September 15, 1997; In Final Form: November 3, 1997

The overtone spectra of adamantane, 1-chloroadamantane, and hexamethylenetetramine have been recorded in various phases and at several temperatures. Phase effects and temperature effects on the overtone spectra are discussed. The vibrational overtone spectra are recorded by conventional near-infrared spectroscopy and by intracavity laser photoacoustic spectroscopy. Peaks corresponding to the nonequivalent CH oscillators of adamantane vapor and 1-chloroadamantane vapor are assigned. Absolute oscillator strengths of adamantane are determined from the conventional spectra, and they are compared with values calculated with a harmonically coupled anharmonic oscillator local mode model and ab initio dipole moment functions. Very good agreement between observed and calculated intensities is obtained.

Introduction

The local mode model of molecular vibration can be used to interpret CH stretching overtone spectra.[1,2] Overtone energies are calculated with a harmonically coupled anharmonic oscillator (HCAO) local mode model.[3−6] Peak positions are sensitive to the CH bond lengths.[7] The shortest CH bonds are expected to correspond to the highest frequency CH stretching oscillator in accord with the frequency bond length correlation.[7] Overtone intensities of reasonable accuracy have been calculated with vibrational wave functions from the HCAO local mode model and ab initio dipole moment functions.[8−14]

The ab initio geometry optimized structures of adamantane, 1-chloroadamantane, and hexamethylenetetramine are depicted in Figure 1, with labels for the nonequivalent CH bonds. In this paper, the focus will be predominantly on adamantane.

Adamantane possesses two solid phases; one phase is orientationally ordered and the other phase is orientationally disordered.[15] At atmospheric pressure and below 208.6 K adamantane exists in the ordered β phase, and above 208.6 K (the α phase) the orientational order is lost. In the high-temperature disordered phase and in the vapor phase there are two types of nonequivalent CH bonds, the methine and methylene. However, in the low-temperature ordered phase of adamantane, there are four types of nonequivalent CH bonds. The nonequivalent CH bonds have been studied with infrared spectroscopy by Corn et al.,[16] who used isotopically dilute $C_{10}D_{15}H$ in a host crystal of perdeuterated adamantane. The phase transition of adamantane has been studied previously by Raman[17,18] and infrared[19] spectroscopy. The Raman and infrared spectra of the low-temperature ordered phase show new factor-group splittings and some new bands.

In the present paper we report the CH stretching overtone spectra of adamantane in the vapor phase, in solution, and in two solid phases. A calculation of the overtone intensities of adamantane is also given. Some overtone spectra of the adamantane analogues, 1-chloroadamantane and hexamethylenetetramine, are presented, and phase effects and temperature effects are examined.

Experimental Section

Crystalline adamantane (Aldrich, 99+%, mp 268 °C) and 1-chloroadamantane (Acros, 98%, mp 163−166 °C) were used without further purification except for degassing, and hexamethylenetetramine (Acros, 99%, unstabilized, mp 250 °C) was used without any further purification.

Vapor-phase spectra of adamantane and 1-chloroadamantane were recorded in the regions corresponding to $\Delta\nu_{CH} = 2$ and 3 with a conventional spectrophotometer (Cary 5e UV−vis−near-IR) that was fitted with a variable path length White cell (Wilks variable path length cell fitted with BK7 Schott glass windows from Melles Griot). Background scans with an evacuated cell were recorded and subtracted for each of the Cary spectra. The spectra in the regions corresponding to $\Delta\nu_{CH} = 4$ and 5 of adamantane and 1-chloroadamantane were recorded with intracavity laser photoacoustic spectroscopy (ICL-PAS). Our version of ICL-PAS has been described elsewhere.[20,21] An argon ion pumped titanium:sapphire solid-state broad band tunable laser (Coherent 890) with mid- and short-wave optics was used for the $\Delta\nu_{CH} = 4$ and 5 regions, respectively. The absolute absorbance is not known with our ICL-PAS apparatus, so we can only obtain relative intensities in the ICL-PAS spectra.[21] The photoacoustic cell contained an electret microphone (Knowles Electronics Inc., EK3132). The cell was filled with Krypton buffer gas at a pressure of 110−165 Torr to increase the photoacoustic signal.[22]

In the room-temperature ICL-PAS spectra of adamantane, water absorptions interfered with the weak adamantane photoacoustic signal. To reduce the amount of water present, a 1:1 mixture of anhydrous $Ca(OH)_2$ and $MgSO_4$ was added to adamantane, and the components were mixed under a N_2 atmosphere. Further drying techniques were used, which have been described previously.[23] The drying agents were not used at elevated temperatures, because the increased temperature would release the water absorbed by the drying agents. The tacky composition of 1-chloroadamantane rendered the use of the drying agents impractical.

The compounds used in this study are relatively nonvolatile. However, with heating, the vapor pressure of the sample may be increased and thus give a stronger signal for a vapor-phase photoacoustic experiment. The elevated temperature depen-

S1089-5639(97)03033-8 CCC: $15.00
Published on Web 01/15/1998

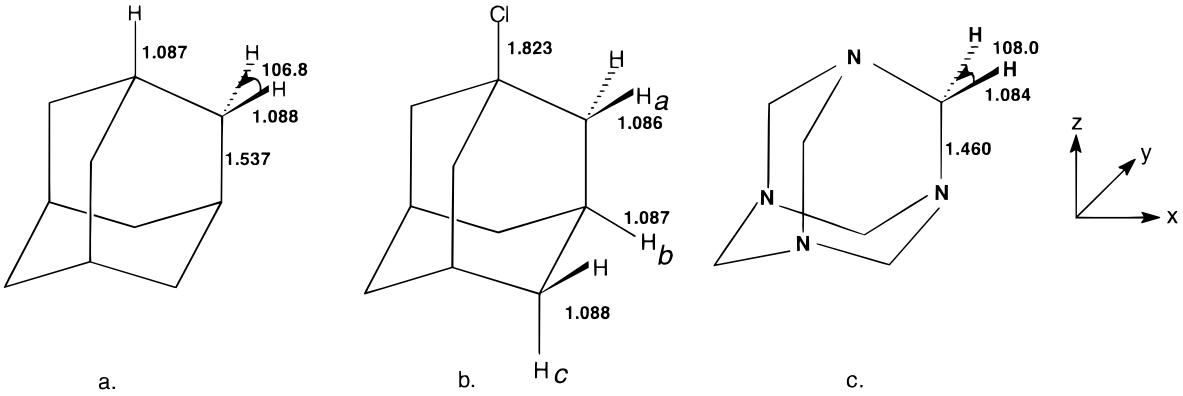

Figure 1. Geometry-optimized structures of (a) adamantane (HF/6-311+G(d,p)), (b) 1-chloroadamantane (HF/6-31G(d,p)), and (c) hexamethylenetetramine (HF/6-31G(d,p)). Bond lengths in angstroms.

dence studies were conducted with a cork insulated oven, constructed of aluminum and consisting of a small heating coil and fan. The temperature was controlled with a Variac and monitored with a mercury thermometer placed through a small hole in the top of the oven. The oven was fitted on the photoacoustic cell holder with the photoacoustic cell already in place, and approximately 20 min was allowed to elapse to reach thermal equilibrium. The temperature remained within ±2 °C during a scan. Hexamethylenetetramine was so nonvolatile that no photoacoustic signal of its vapor could be detected.

Adamantane and 1-chloroadamantane were dissolved in CCl_4 to produce 0.50 and 0.60 M solutions, respectively. Spectra of these solutions were recorded in 10-cm quartz cells with CCl_4 in a 10-cm reference cell on the Cary spectrophotometer at room temperature. A suitable solvent for hexamethylenetetramine could not be found. We found that hexamethylenetetramine was only readily soluble in solvents that contained XH bonds, and thus the solvent band intensities overwhelmed the weaker hexamethylenetetramine absorption.

The overtone spectra of the three adamantane solids were recorded on the Cary with a 2-mm quartz cuvette at room temperature. For the reduced temperature studies, the quartz cuvette was placed inside a variable-temperature liquid nitrogen cryostat (Oxford Instruments model DN704) with air as a reference. The temperature was measured with a type K nickel−chromium versus nickel−aluminum thermocouple. The solid-phase spectra had relatively high absorbance baselines due to light scattering by the samples, so a light attenuator was used in the reference beam path to lower the baseline absorbance. The spectral bandwidth (slitwidth) of the Cary was preset to 1.5 nm to ensure good resolution and a high signal-to-noise ratio.

The overtone spectra were decomposed with a deconvolution program in Spectra Calc.[24] The spectra were deconvoluted into a number of Lorentzian peaks and a linear baseline. The deconvolution yields peak positions, areas, and bandwidths. Uncertainty in the deconvolution is highly dependent on peak resolution. For well-resolved peaks, we typically estimate the uncertainty to be less than 5 cm^{-1} for peak positions and less than 10% for intensities. However, for the poorly resolved peaks in the adamantanes, we estimate a higher uncertainty, on the order of 10 cm^{-1} for peak positions and 50% for intensities. Bandwidths are given as the full width at half-maximum (fwhm).

Theory

Overtone intensities are generally reported as the dimensionless quantity, oscillator strength, *f*. The oscillator strength of a transition from the ground vibrational state *g* to an excited vibrational state *e* is given by[10,25]

$$f = 4.702 \times 10^{-7}\ [\mathrm{cm}^{-1}\ \mathrm{D}^{-2}]\tilde{\nu}_{eg}|\vec{\mu}_{eg}|^2 \qquad (1)$$

where $\tilde{\nu}_{eg}$ is the transition frequency in cm^{-1} and $\vec{\mu}_{eg} = \langle e|\vec{\mu}|g\rangle$ is the transition dipole moment in debyes. We obtained experimental solution-phase adamantane oscillator strengths with the expression[25,26]

$$f = 4.3192 \times 10^{-12}\ (\mathrm{mol\ cm}^{-1})\frac{9n}{(n^2+2)^2}\frac{1}{cl}\int A_{\mathrm{liq}}(\tilde{\nu})\,\mathrm{d}\tilde{\nu} \qquad (2)$$

where *n* is the refractive index of the liquid (CCl_4), *c* is the molar concentration, *l* is the path length, and A_{liq} is the absorbance of the solution. It has been assumed that the refractive index of CCl_4 ($n = 1.4601$)[27] is unchanged with the addition of adamantane.

Adamantane has four equivalent methine hydrogens and 12 equivalent methylene hydrogens. The coupling between the methine and methylene hydrogens will be small, since they are attached to different carbon atoms.[12,28] We use the local mode theory of harmonically coupled anharmonic oscillators (HCAO) and neglect this small coupling. Thus we treat adamantane as nonequivalent isolated methine and methylene groups, with each CH bond described by a Morse oscillator. A brief outline of the model used to calculate the intensities of the methine oscillator is presented, and we refer to recent papers for an analysis of the HCAO local mode model and the procedures used to determine ab initio dipole moment functions for the methylene group.[10−13]

The zeroth-order Hamiltonian for the methine CH group can be written as[29]

$$(H^0 - E^0_{|0\rangle})/hc = \upsilon_a\tilde{\omega}_a - (\upsilon_a{}^2 + \upsilon_a)\upsilon_a\tilde{\omega}_a x_a \qquad (3)$$

where $\tilde{\omega}_a$ and $\tilde{\omega}_a x_a$ are the local mode frequency and anharmonicity of the methine CH_a oscillator. $E^0_{|0\rangle}$ is the zeroth-order energy of the ground state. The eigenstates for the methine group can be written as $|\upsilon_a\rangle$, where υ_a is the quantum number of vibrational excitation in the methine oscillator. These eigenstates are Morse oscillator wave functions.

The dipole moment function is given in our approximation as a series expansion in the internal CH displacement coordinate, *q*. For a methine CH oscillator, we have

$$\vec{\mu}(q) = \sum_i \vec{\mu}_i q^i \qquad (4)$$

where

$$\vec{\mu}_i = \frac{1}{i!}\frac{\partial^i \vec{\mu}}{\partial q_a^i}\bigg|_e \tag{5}$$

We limit the expansion in eq 4 to fourth-order terms.[11] Ab initio molecular orbital theory is used to calculate dipole moment values at geometries in which one of the CH bonds is displaced from equilibrium. This provides one-dimensional grids of the dipole moment as a function of q and allows us to determine the coefficients $\vec{\mu}_i$.

Intramanifold coupling between oscillators bonded to the same carbon, as in a methylene group, is significant.[10] The perturbation is

$$\frac{H'_{\text{intra}}}{hc} = -\sum_{b\neq c}\gamma'_{bc}(a_b a_c^+ + a_b^+ a_c) \tag{6}$$

with the coupling parameters

$$\gamma'_{bc} = (\gamma_{bc} - \phi_{bc})\sqrt{\tilde{\omega}_b \tilde{\omega}_c} \tag{7}$$

where a^+ and a are step up and step down operators,[30] respectively, and the indices b and c refer to the methylene CH bonds.

The parameters γ and ϕ are defined by[3]

$$\gamma_{bc} = -\frac{1}{2}\frac{G^\circ_{bc}}{\sqrt{G^\circ_{bb}G^\circ_{cc}}} = -\frac{\cos\theta}{2}\left(1 + \frac{m_{\text{c}}}{m_{\text{H}}}\right)^{-1} \tag{8}$$

and

$$\phi_{bc} = \frac{1}{2}\frac{F_{bc}}{\sqrt{F_{bb}F_{cc}}} \tag{9}$$

where the G°_{nm} are the Wilson **G**-matrix elements,[31] θ is the HCH bond angle, and m_{C} and m_{H} are the C and H atomic masses, respectively. The F_{nm} are the force constant parameters. The γ' parameter represents the coupling strength between oscillators. Within this approximation, the γ' (intramanifold) term couples two states within the same manifold. The kinetic term, γ , depends only on the **G** matrix and thus only on the geometry and composition of the XH_n group, while the potential term ϕ depends only on the force constant, F_{nm}, which can be obtained from an ab initio calculation. Alternatively, γ'_{bc} can be approximated directly from the spectra (vide infra).

All of the ab initio calculations used Gaussian 92.[32] Intensities were calculated with dipole moment grids that were generated at the self-consistent-field Hartree−Fock (HF) level with the STO-3G, 6-31G(d), and 6-311+G(d,p) standard basis sets.

Results and Discussion

The local mode theory of molecular vibration is used to explain the CH stretching overtone spectra of the adamantanes. A single peak is expected for each nonequivalent CH bond. On the basis of the local mode model, we would expect two peaks in the adamantane overtone spectrum corresponding to the methine and methylene CH bonds. For 1-chloroadamantane there are four nonequivalent CH bonds. However, the HF/6-31G(d,p) geometry optimization gives only three different CH bond lengths. The nonequivalent methylene CH bonds labeled CH_c are not expected to be resolved due to their equivalent bond lengths. For hexamethylenetetramine only one peak is predicted, since it contains six equivalent methylene groups.

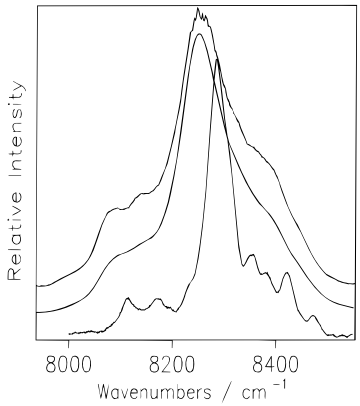

Figure 2. Room-temperature overtone spectra of adamantane solid (top), 0.50 M solution (middle), and vapor (~0.2 Torr) in the $\Delta v_{\text{CH}} = 3$ region measured with path lengths of 2 mm (solid), 10 cm (solution), and 20.25 m (vapor).

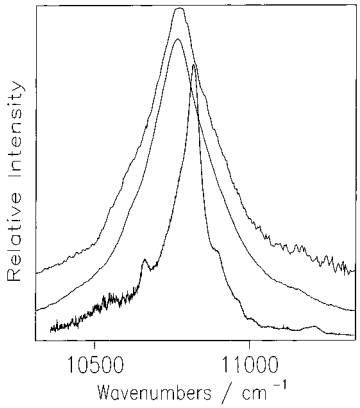

Figure 3. Room-temperature overtone spectra of adamantane solid (top), 0.50 M solution (middle), and vapor (~0.2 Torr) in the $\Delta v_{\text{CH}} = 4$ region measured with path lengths of 2 mm (solid) and 10 cm (solution). The vapor-phase spectrum was measured by ICL-PAS in the presence of 165 Torr of Kr buffer gas.

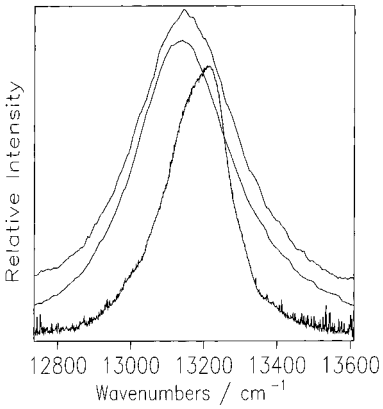

Figure 4. Room-temperature overtone spectra of adamantane solid (top), 0.50 M solution (middle), and vapor (~0.2 Torr) in the $\Delta v_{\text{CH}} = 5$ region measured with path lengths of 2 mm (solid) and 10 cm (solution). The vapor-phase spectrum was measured by ICL-PAS in the presence of 110 Torr of Kr buffer gas.

Phase Effects. The overtone spectra of adamantane in the regions corresponding to $\Delta v_{\text{CH}} = 3-5$ are presented in Figures 2−4. The observed frequencies of the adamantane pure local mode peaks $|v0\rangle_\pm$ and $|v\rangle$, which represent the methylene and methine CH bonds, respectively, are shown in Table 1 along with the observed frequencies of the combination bands. The

TABLE 1: Observed Frequencies (cm^{-1}) and Peak Assignments in the Room-Temperature Overtone Spectra of Adamantane in Various Phases

assignment	vapor	solid	in CCl_4
combination	5529		5472
combination	5572		5510
$\|20\rangle_+$	5646		5555
$\|20\rangle_-$	5691		5624
$\|2\rangle$	5707		5679
$\|11\rangle$	5808		5782
combination	5843		5804
combination	8114		8086
combination	8169		8135
$\|30\rangle_\pm$	8284	8245	8246
$\|3\rangle$	8310	8286	8294
combination	8354		
combination	8382	8387	8385
combination	8422		
combination	8473		
combination	10 544		
combination	10 661		
$\|40\rangle_\pm$	10 776	10 769[a]	10 768[a]
$\|4\rangle$	10 820		
combination	10 902		
$\|50\rangle_\pm$	13 159	13 149[a]	13 140[a]
$\|5\rangle$	13 228		

[a] Only one peak was resolved in these regions.

TABLE 2: Local Mode Parameters (cm^{-1}) of Adamantane in Various Phases

	$\tilde{\omega}$	$\tilde{\omega}x$	$\tilde{\omega}$	$\tilde{\omega}x$
vapor	3021 ± 7^a	65.1 ± 1.3^a	3019 ± 9^b	62.4 ± 1.7^b
0.5 M in CCl_4	2991 ± 11^c	60.3 ± 2.1^c		
solid	2986 ± 9^c	59.2 ± 1.8^c		

[a] Parameters for the methylene group. [b] Parameters for the methine group. [c] Parameters obtained by fitting the single peaks of $\Delta v_{CH} = 4$ and 5 with $|30\rangle_\pm$.

frequencies $\tilde{\nu}$ of the local mode peaks ($|v0\rangle_\pm$ and $|v\rangle$) have been fitted to a two-parameter Morse oscillator energy expression

$$\tilde{\nu}/v = \tilde{\omega} - (v+1)\tilde{\omega}x \qquad (10)$$

in order to obtain values of the local mode frequency $\tilde{\omega}$ and anharmonicity $\tilde{\omega}x$ of the two nonequivalent CH oscillators. The local mode parameters of adamantane in various phases are given in Table 2.

The ab initio geometry optimization of adamantane has a methine CH bond length 0.001 Å shorter than the methylene bonds. Thus, with this difference in bond length, we would expect to resolve two peaks in the overtone spectra, with the shorter methine having the higher frequency. Inspection of the overtone spectra shows that in the vapor phase there are two overlapping peaks due to the methylene and methine CH bonds. The higher overtones in the solid and solution give rise to one broad peak; this is to be expected because of the similar bond lengths of the methylene and methine groups and the typical line shape broadening that occurs in solid and solution.

The local mode parameters indicate the transition from vapor to solid causes a significant decrease in the local mode frequency $\tilde{\omega}$. Generally, an increase in dispersive forces (attractive forces between molecules) results in a lowering (red shift) of fundamental vibrational frequencies. The increase in intermolecular attractive forces in the condensed phase will lead to a decrease in the intramolecular CH bond strength and thus to slightly lower CH stretching frequencies. There is ample experimental data for this red shift of fundamental CH stretching frequencies.[33] The red shift is observed between the solid[34] and vapor[16] fundamentals of adamantane, and we observe it in the overtone regions as well. The shift is clearly depicted in Table 1, where the positions of the condensed-phase peaks lie lower in energy than the vapor-phase peaks.

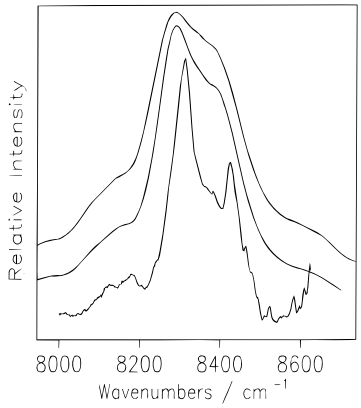

Figure 5. Room-temperature overtone spectra of 1-chloroadamantane solid (top), 0.60 M solution (middle), and vapor in the $\Delta v_{CH} = 3$ region measured with path lengths of 2 mm (solid), 10 cm (solution), and 23.25 m (vapor).

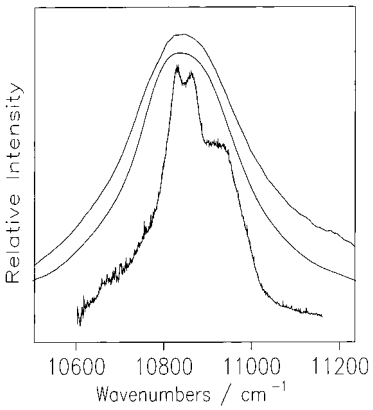

Figure 6. Room-temperature overtone spectra of 1-chloroadamantane solid (top), 0.60 M solution (middle), and vapor in the $\Delta v_{CH} = 4$ region measured with path lengths of 2 mm (solid) and 10 cm (solution). The vapor-phase spectrum was measured by ICL-PAS in the presence of 120 Torr of Kr buffer gas.

There is a decrease in the anharmonicity $\tilde{\omega}x$ for the condensed phases relative to the vapor. This trend is in agreement with the behavior of viscosity-dependent barriers as described by Dellinger and Kasha.[35] Dellinger and Kasha proposed that as the viscosity of the medium increased, intermolecular perturbations will also be increased, and the movement of the oscillators in the higher viscosity medium would be more restricted, leading to a more harmonic vibrational potential.

1-Chloroadamantane. The overtone spectra of 1-chloroadamantane in the regions corresponding to $\Delta v_{CH} = 3-5$ are given in Figures 5−7. The observed frequencies and assignments of the vapor-phase overtone transitions are listed in Table 3. The labeling of the transitions follows the labels of the CH oscillators in the geometry-optimized structure of 1-chloroadamantane (Figure 1). The shifts in the overtone peak positions between the vapor and the other two states are presented in Table 4. Similar to adamantane, all of the condensed-phase transitions of 1-chloroadamantane are red-shifted relative to the vapor-phase transitions.

In the vapor-phase $\Delta v_{CH} = 4$ and 5 regions, three overlapping peaks are observed corresponding to the three different CH oscillators. The assignments are consistent with the predictions based on the HF/6-31G(d,p) geometry optimization. Like

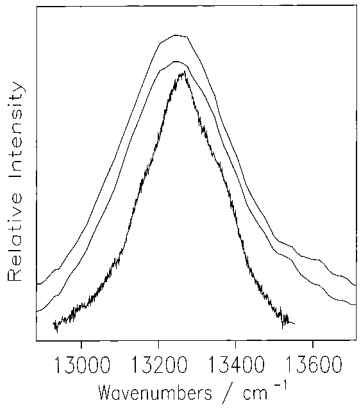

Figure 7. Room-temperature overtone spectra of 1-chloroadamantane solid (top), 0.60 M solution (middle), and vapor in the $\Delta v_{CH} = 5$ region measured with path lengths of 2 mm (solid) and 10 cm (solution). The vapor-phase spectrum was measured by ICL-PAS in the presence of 115 Torr of Kr buffer gas.

TABLE 3: Observed Frequencies (cm^{-1}) and Peak Assignments in the Room-Temperature Vapor-Phase Overtone Spectrum of 1-Chloroadamantane[a]

assignment	frequency	assignment	frequency
$\|20\rangle_{c\pm}$	5701	combination	10 755
$\|2\rangle$ with $\|20\rangle_{a\pm}$	5723	$\|40\rangle_{c\pm}$	10 827
combination	5817	$\|4\rangle$	10 867
combination	5835	$\|40\rangle_{a\pm}$	10 917
combination	5861	combination	10 956
combination	5884		
		$\|50\rangle_{c\pm}$	13 166
combination	8126	$\|5\rangle$	13 260
combination	8180	$\|50\rangle_{a\pm}$	13 365
combination	8280		
$\|30\rangle_{c\pm}$	8311		
$\|3\rangle$	8368		
$\|30\rangle_{a\pm}$	8430		

[a] See Figure 1 for definitions of the *a* and *c* CH bond labels.

TABLE 4: Shifts in Overtone Peak Positions (cm^{-1}) between Different Phases of 1-Chloroadamantane

state	$\tilde{\nu}_{vapor} - \tilde{\nu}_{solid}$	$\tilde{\nu}_{vapor} - \tilde{\nu}_{solution}$
$\|30\rangle_a$	+53	+33
$\|3\rangle$	+51	+36
$\|30\rangle_c$	+30	+25
$\|4\rangle$	+17	+19
$\|5\rangle$	+17	+14

adamantane, in the $\Delta v_{CH} = 4$ and 5 regions of the solid and solution, only one broad peak is observed. Thus a fit of three peaks to eq 10 could not be performed with the solid and solution. However, a fit was made of the methine peak in the $\Delta v_{CH} = 3$ region with the single bands in the $\Delta v_{CH} = 4$ and 5 regions. This is a reasonable assumption, because the methine bond length is the average bond length for the CH oscillators of 1-chloroadamantane and consequently it is energetically predicted to lie between the two different methylene peaks. The local mode parameters of 1-chloroadamantane are given in Table 5. The local mode frequency $\tilde{\omega}$ and anharmonicity $\tilde{\omega}x$ decreased by approximately 48 and 8 cm^{-1}, respectively, on the passage from vapor to solid. As with adamantane, we attribute the decrease in $\tilde{\omega}$ to an increase in dispersive forces in the condensed phase and the decrease in $\tilde{\omega}x$ to a solvent matrix perturbation.

Temperature Effects: Solid Phase. The overtone spectra of adamantane in the $\Delta v_{CH} = 3-5$ regions in the ordered and disordered phases are shown in Figures 8−10. In the $\Delta v_{CH} = 3$ region, the low-temperature (ordered phase) spectrum is much sharper and better resolved than the room-temperature spectrum. In the room-temperature spectrum, the methylene local mode peak is centered at 8245 cm^{-1}, with a higher energy shoulder due to the methines at 8286 cm^{-1}. In the low-temperature ordered phase, there is a significant change in this region. A definite trio of CH stretching local mode peaks appearing at 8230 cm^{-1} (peak I), 8261 cm^{-1} (peak II), and 8308 cm^{-1} (peak III) are observed. Peak III contains a low-energy shoulder, which is assigned as the fourth CH stretching local mode peak. The low-energy shoulder was not well-resolved, so when a peak was assigned to it in Spectra Calc the deconvolution gave unrealistic results; that is, it produced peaks that were obviously too broad. However, the assignment of the shoulder as a pure local mode transition appears to be valid since the intensity of peak III with the shoulder is twice that of peak I or peak II. To a zeroth-order approximation, we would expect the four nonequivalent CH oscillators of the ordered phase to have the same intensity.

Corn et al.[16] assigned the lowest frequency CH stretching band in the fundamental region of the low-temperature ordered phase of adamantane to the methine group with the aid of a deuterated analogue. In the absence of overtone studies of deuterated analogues of adamantane, it is not possible for us to make definitive assignments of this type.

The solid-phase $\Delta v_{CH} = 4$ and 5 regions of adamantane are interesting. In both regions, the overall bandwidth of the lower temperature samples is greater than the room-temperature counterpart (approximately 109 and 49 cm^{-1} wider for the $\Delta v_{CH} = 4$ and 5 regions, respectively). The increase in width is opposite to the usual narrowing that occurs with a decrease in temperature. The broadening of the overtone regions in adamantane occurs because the increased number of nonequivalent CH bonds in the low-temperature ordered phase leads to a greater splitting between the local mode peaks. The low-temperature solid-phase spectra are not well-resolved, but a trio of peaks are observed in the $\Delta v_{CH} = 4$ region and the wide shoulders of the $\Delta v_{CH} = 5$ band provide evidence of the extra nonequivalent CH stretching local modes. Local mode parameters were not calculated for the CH oscillators of the low-temperature adamantane sample due to the low resolution of the local mode peaks.

The room-temperature and cryogenic solid-phase overtone spectra of 1-chloroadamantane corresponding to the $\Delta v_{CH} = 3-5$ regions are shown in Figures 11−13. 1-Chloroadamantane undergoes an order−disorder transition at 244.2 K;[36] however no information was found in the literature regarding the molecular orientation in the low-temperature ordered phase. The 1-chloroadamantane $\Delta v_{CH} = 3-5$ overtone regions were recorded at 90 K. Besides the narrowing of the low-intensity combination bands, broadening of the local mode peaks between 8294 and 8461 cm^{-1} in the low temperature $\Delta v_{CH} = 3$ region is observed in comparison to the room-temperature spectrum. The line shapes and line widths between the ordered and disordered phases of 1-chloroadamantane in the $\Delta v_{CH} = 4$ and 5 regions are unchanged within experimental error. The room-temperature overtones are red-shifted in relation to the low-temperature overtones. For example, the $|30\rangle_{c\pm}$ local mode peak in the room-temperature spectrum lies 30 cm^{-1} lower in energy than in the low-temperature spectrum. A similar red shift is observed in the $\Delta v_{CH} = 4$ and 5 regions, in which the room-temperature peaks are red-shifted by 33 and 43 cm^{-1}, respectively. The red shift indicates the CH bonds of 1-chloroadamantane are weakened more by dispersion forces in the disordered phase.

TABLE 5: Local Mode Parameters of 1-Chloroadamantane in Various Phases[a]

	CH_c		CH_b		CH_a	
	$\tilde{\omega}$	$\tilde{\omega}x$	$\tilde{\omega}$	$\tilde{\omega}x$	$\tilde{\omega}$	$\tilde{\omega}x$
vapor	3063 ± 11	71.7 ± 2.3	3069 ± 6	69.9 ± 1.2	3058 ± 18	64.5 ± 4.0
solution			3033 ± 4	64.1 ± 0.7		
solid			3020 ± 6	61.9 ± 1.2		

[a] The single peaks observed for the $\Delta v_{CH} = 4$ and 5 overtones of the solution and solid were treated as methine peaks (see text).

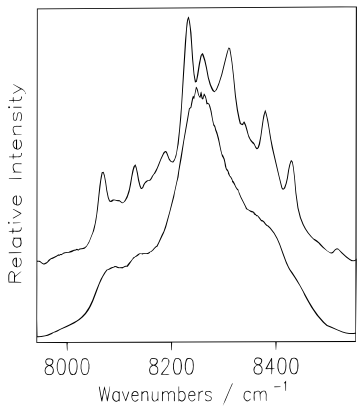

Figure 8. Overtone spectra of 113 K (ordered phase) adamantane solid (top) and room-temperature solid (disordered phase) in the $\Delta v_{CH} = 3$ region measured with a path length of 2 mm.

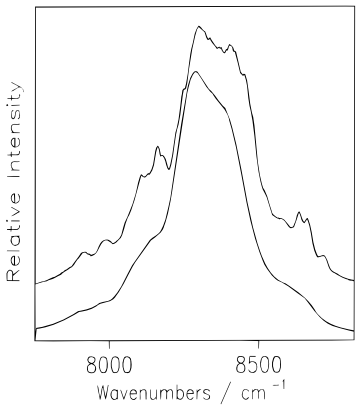

Figure 11. Overtone spectra of 90 K (ordered phase) 1-chloroadamantane solid (top) and room-temperature solid (disordered phase) in the $\Delta v_{CH} = 3$ region measured with a path length of 2 mm.

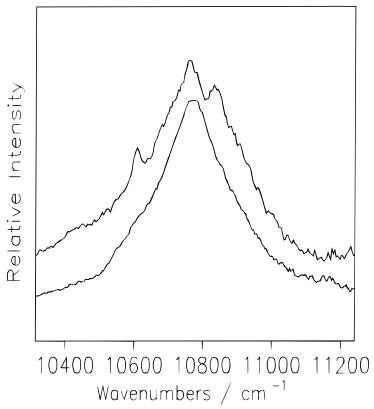

Figure 9. Overtone spectra of 113 K (ordered phase) adamantane solid (top) and room-temperature solid (disordered phase) in the $\Delta v_{CH} = 4$ region measured with a path length of 2 mm.

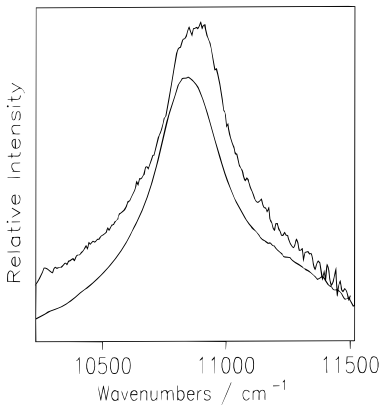

Figure 12. Overtone spectra of 90 K (ordered phase) 1-chloroadamantane solid (top) and room-temperature solid (disordered phase) in the $\Delta v_{CH} = 4$ region measured with a path length of 2 mm.

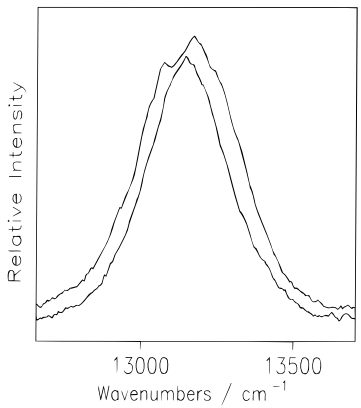

Figure 10. Overtone spectra of 113 K (ordered phase) adamantane solid (top) and room-temperature solid (disordered phase) in the $\Delta v_{CH} = 5$ region measured with a path length of 2 mm.

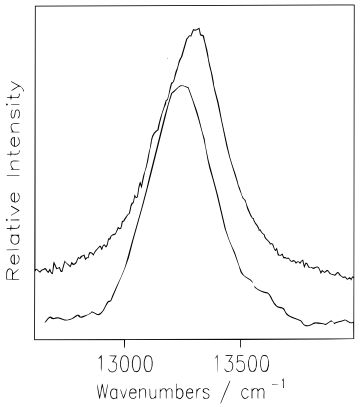

Figure 13. Overtone spectra of 90 K (ordered phase) 1-chloroadamantane solid (top) and room-temperature solid (disordered phase) in the $\Delta v_{CH} = 5$ region measured with a path length of 2 mm.

The room-temperature and cryogenic (113 K) solid-phase overtone spectra of hexamethylenetetramine corresponding to the $\Delta v_{CH} = 3-5$ regions are shown in Figures 14−16. The $\Delta v_{CH} = 3$ region is more complicated for hexamethylenetetramine than for either adamantane or 1-chloroadamantane. The more complicated profile is unexpected because hexamethylenetetramine only has methylene groups, as opposed to the methylene and methine groups possessed by adamantane and

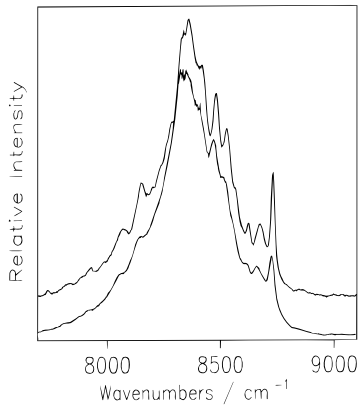

Figure 14. Overtone spectra of 113 K hexamethylenetetramine solid (top) and room-temperature solid in the $\Delta v_{CH} = 3$ region measured with a path length of 2 mm.

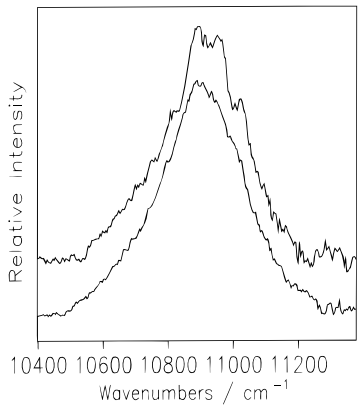

Figure 15. Overtone spectra of 113 K hexamethylenetetramine solid (top) and room-temperature solid in the $\Delta v_{CH} = 4$ region measured with a path length of 2 mm.

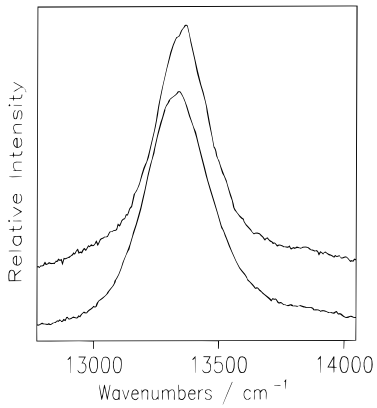

Figure 16. Overtone spectra of 113 K hexamethylenetetramine solid (top) and room-temperature solid in the $\Delta v_{CH} = 5$ region measured with a path length of 2 mm.

1-chloroadamantane. While the room-temperature $\Delta v_{CH} = 3$ solid-phase overtone spectra of adamantane and 1-chloroadamantane have relatively smooth band profiles, the spectrum of hexamethylenetetramine has many sharp combination peaks on the high-energy side of the $\Delta v_{CH} = 3$ band. However, as with the other adamantanes, only one peak is observed in the $\Delta v_{CH} = 4$ and 5 overtone regions of hexamethylenetetramine, although some residual structure is present in the low temperature spectrum at $\Delta v_{CH} = 4$.

The room-temperature $|30\rangle_{\pm}$ peak of hexamethylenetetramine at 8334 cm^{-1} was fitted to eq 10 to the lone $\Delta v_{CH} = 4-5$ bands to yield the local mode parameters $\tilde{\omega} = 2998 \pm 9$ cm^{-1} and

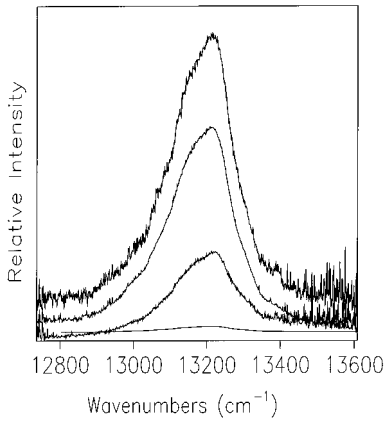

Figure 17. Vapor phase photoacoustic overtone spectra of adamantane in the $\Delta v_{CH} = 5$ region at 87, 78, 57, and 24 °C from top to bottom, respectively. The spectra were measured by ICL-PAS in the presence of 110 Torr of Kr buffer gas.

$\tilde{\omega}x = 54.7 \pm 1.7$ cm^{-1}. The local mode frequency of solid hexamethylenetetramine is similar to the local mode frequencies of the two other solid adamantanes, but the anharmonicity is comparatively lower (54.7 cm^{-1} compared with 61.9 cm^{-1} for 1-chloroadamantane and 60.3 cm^{-1} for adamantane).

Lowering the temperature of hexamethylenetetramine resulted primarily in a sharpening of the combination bands in the $\Delta v_{CH} = 3$ region. In the $\Delta v_{CH} = 4$ region, there was a slight increase in structure, but the overall bandwidth remained the same at both temperatures. For $\Delta v_{CH} = 5$, the low-temperature bandwidth is narrower by about 50 cm^{-1}.

Temperature Effects: Vapor Phase. The vapor-phase photoacoustic spectra of adamantane recorded at various temperatures in the $\Delta v_{CH} = 5$ region are shown in Figure 17. Heating nonvolatile samples can be advantageous because it raises the vapor pressure and hence provides an increased signal. An increase in signal-to-noise is especially important when dealing with CH stretching overtones, which are intrinsically very weak transitions. We have observed that the sensitivity of the microphone rapidly decreases above 130 °C, so spectra recorded above this temperature are unreliable. It has been proposed that some overtone bands that have in the past been assigned as combination bands due to nonequivalent oscillators may actually be hot bands.[37] No hot bands were observed under the mild heating conditions of this study.

Adamantane Overtone Intensities. The dipole moment function, the vibrational energies, and the vibrational wave functions are required to calculate overtone intensities (see eq 1). For the vibrational part of the intensity calculation, the HCAO model is used with only three parameters: the local mode frequency, $\tilde{\omega}$, the local mode anharmonicity, $\tilde{\omega}x$, and the intramanifold coupling term, γ'. All three parameters can be obtained from the observed spectra, or alternatively, γ' can be obtained from an ab initio calculation. Intensities with γ' calculated ab initio and from experimental results will be presented and compared. Note that none of these parameters are chosen on the basis of fitting the observed intensity data.

The dipole moment function is generated from ab initio calculations. As expected, the calculated dipole moment of adamantane in its equilibrium geometry was zero. Dipole moment grids were calculated for adamantane at the HF level with the STO-3G, 6-31G(d), and 6-311+G(d,p) basis sets with the Gaussian 92 ab initio molecular orbital program. The notation $\vec{\mu}_a$ and $\vec{\mu}_{bc}$ has been used, where the letter a in $\vec{\mu}_a$ refers to the methine CH bond and the letters b and c in $\vec{\mu}_{bc}$ refer to

TABLE 6: *Ab Initio* HF/6-311+G(d,p) Dipole Moment Derivative Expansion Coefficients for Methine (*a*) and Methylene (*b, c*) CH Bonds in Adamantane[a]

$\vec{\mu}_a$	z	$\vec{\mu}_{bc}$	x	y	z
$\vec{\mu}_1$/D Å^{-1}	−1.333 26	$\vec{\mu}_{10}$/D Å^{-1}	−0.728 87	0.805 06	−0.515 39
$\vec{\mu}_2$/D Å^{-2}	−2.104 86	$\vec{\mu}_{20}$/D Å^{-2}	−1.053 20	1.066 92	−0.744 73
$\vec{\mu}_3$/D Å^{-3}	−0.486 70	$\vec{\mu}_{30}$/D Å^{-3}	−0.230 30	0.161 53	−0.162 86
$\vec{\mu}_4$/D Å^{-4}	0.177 34	$\vec{\mu}_{40}$/D Å^{-4}	0.114 19	0.162 11	0.081 02
		$\vec{\mu}_{11}$/D Å^{-2}	0.536 04	0.000 00	0.379 03
		$\vec{\mu}_{21}$/D Å^{-3}	0.261 04	0.356 85	0.184 62

[a] The indices refer to the order of the expansion coefficients (see eq 5) for methine. For methylene,

$$\vec{\mu}_{ij} = \frac{1}{i!j!}\frac{\partial^{i+j}\vec{\mu}}{\partial q_b^i\,\partial q_c^j}\bigg|_e$$

the respective CH bonds in the methylene group. The derivative coefficients for the methylene group were calculated from an *ab initio* 7 × 7 grid with a stepsize of 0.1 Å between the grid points (maximum displacements from equilibrium of ±0.3 Å). Only the upper triangle of the grid points plus the diagonal was necessary because of the equivalence of the methylene CH oscillators; that is, 28 points were calculated instead of 49. For the methine CH, a 1-D grid of 7 points was computed with the same stepsize and displacements. The HF/6-311+G(d,p) dipole moment expansion coefficients for the methine and methylene CH bonds are given in Table 6.

The dipole moment expansion coefficients for the methine and methylene CH bonds have characteristics similar to those that have been noted previously for other molecules.[11,38] That is, the magnitude of the diagonal terms fall in the order second > first ≫ third. Thus higher than linear terms in the dipole moment function are essential if accurate overtone intensities are sought. The relative magnitudes of the methine dipole moment derivatives are greater than the corresponding methylene derivatives. This suggests that the methine CH oscillator will have a greater intrinsic intensity than a methylene CH. Of course, the greater number of methylene oscillators will undoubtedly lead to a greater overall methylene intensity in the overtone spectra. The *z* axis has been selected to pass through the methine CH bond and the *xz* plane bisects the methylene HCH angle, as shown in Figure 1. Note that in this axis system the *y* component of $\vec{\mu}_{11}$ is expected to be zero by symmetry.

A value for the effective intramanifold coupling term γ_{bc}' was calculated with Gaussian 92. The kinetic part, γ_{bc} (eq 8), is determined by the geometry of the HCH fragment (**G**-matrix elements), and the potential part, ϕ_{bc}, by the relevant force constants. The angle HCH was determined to be 106.8° from the geometry optimization. Calculation of the force constants in internal coordinates yielded $F_{bb} = F_{cc} = 0.363\,986$ au and $F_{bc} = 4.49904 \times 10^{-3}$ au (hartree/bohr^2). The value $\gamma_{bc}' = 15$ cm^{-1} was obtained from eq 7 with the values of γ_{bc} and ϕ_{bc} and the experimental local mode frequency $\tilde{\omega}$. The coupling parameter of 15 cm^{-1} is the same value as that calculated for the similar molecule cyclohexane.[11] It is also possible to provide direct experimental evidence to compare with the calculated value of γ_{bc}'. For an XH_2 group with similar bonds, the splitting between the symmetric and antisymmetric CH stretching states of the fundamental is equal to twice the intramanifold coupling constant in the HCAO local mode model under the assumption that these fundamentals are not perturbed through interactions with other states corresponding to different types of vibrational motion.[8,9] The frequencies of the fundamental asymmetric CH_2 stretch and symmetric CH_2 stretch, as reported by Broxton *et al.*,[39] were 2929 and 2850 cm^{-1}, respectively. Mecke et al.[34] reported frequencies of 2933 and 2857 cm^{-1}. The average of these splittings was used to give a value of $\gamma_{bc}' = 39$ cm^{-1}. This value is considerably higher than the ab initio value of 15 cm^{-1}. Intensity calculations were performed with both values of γ_{bc}' to examine its effect on the oscillator strengths.

TABLE 7: Calculated Frequencies (cm^{-1}) and Oscillator Strengths, *f*, for CH Stretching of the Six Methylene Groups of Adamantane at the HF/6-311+G(d,p) Level[a]

	frequency		*f*	
state	$\gamma_{bc}' = 15$	$\gamma_{bc}' = 39$	$f_{\gamma' bc=15}$	$f_{\gamma' bc=39}$
$\|20\rangle_+$	5645	5615	2.1×10^{-7}	9.0×10^{-8}
$\|11\rangle$	5788	5818	4.3×10^{-7}	5.5×10^{-7}
$\|20\rangle_-$	5651	5651	1.6×10^{-7}	1.6×10^{-7}
total			8.0×10^{-7}	8.0×10^{-7}
$\|30\rangle_+$	8279	8260	6.8×10^{-8}	5.7×10^{-8}
$\|21\rangle_+$	8515	8486	6.7×10^{-9}	1.8×10^{-8}
$\|21\rangle_-$	8574	8633	5.1×10^{-9}	8.5×10^{-9}
$\|30\rangle_-$	8279	8268	4.2×10^{-8}	3.8×10^{-8}
total			1.2×10^{-7}	1.2×10^{-7}
$\|40\rangle_+$	10 780	10 766	7.0×10^{-9}	6.6×10^{-9}
$\|31\rangle_+$	11 156	11 101	1.4×10^{-10}	4.8×10^{-10}
$\|22\rangle$	11 321	11 390	1.0×10^{-11}	7.9×10^{-11}
$\|31\rangle_-$	11 175	11 188	4.7×10^{-10}	9.4×10^{-10}
$\|40\rangle_-$	10 780	10 767	6.0×10^{-9}	5.6×10^{-9}
total			1.4×10^{-8}	1.4×10^{-8}
$\|50\rangle_+$	13 150	13 137	7.2×10^{-10}	7.0×10^{-10}
$\|50\rangle_-$	13 150	13 137	9.1×10^{-10}	8.6×10^{-10}
total			1.7×10^{-9}	1.7×10^{-9}
$\|60\rangle_+$	15 390	15 378	8.4×10^{-11}	8.2×10^{-11}
$\|60\rangle_-$	15 390	15 378	1.5×10^{-10}	1.5×10^{-10}
total			2.4×10^{-10}	2.4×10^{-10}
$\|70\rangle_+$	17 499	17 488	1.1×10^{-11}	1.1×10^{-11}
$\|70\rangle_-$	17 499	17 488	2.9×10^{-11}	2.8×10^{-11}
total			4.1×10^{-11}	4.1×10^{-11}

[a] Combination states for $v > 4$ are omitted, but their oscillator strengths are included in the totals.

TABLE 8: Calculated Frequencies (cm^{-1}) and Oscillator Strengths for CH Stretching of the Four Methine Groups of Adamantane at the HF/6-311+G(d,p) Level

state	frequency	*f*
$\|2\rangle$	5664	4.6×10^{-7}
$\|3\rangle$	8308	7.3×10^{-8}
$\|4\rangle$	10 828	6.6×10^{-9}
$\|5\rangle$	13 223	6.4×10^{-10}
$\|6\rangle$	15 493	7.2×10^{-11}
$\|7\rangle$	17 639	9.4×10^{-12}

The mixing of pure local mode states into the combination states usually increases with increasing γ'. In other words, the intensities of pure local mode states will decrease slightly, while combination peaks such as $|31\rangle_+$ and $|22\rangle$ will increase with larger values of γ'. The mixing of states generally decreases with increasing vibrational levels v, since the effective coupling decreases with increasing v. It should be noted that changes in γ' will only change the distribution of intensity between states; the total oscillator strength of a manifold will remain unchanged.

The calculated frequencies and oscillator strengths of the $\Delta v_{CH} = 2-7$ overtones associated with the six methylene groups of adamantane and calculated at the HF/6-311+G(d,p) level are shown in Table 7. Combination states for manifolds $v > 4$ are omitted because they are several orders of magnitude less intense than the pure local mode states $|v0\rangle_\pm$ and $|v\rangle$, and they are not observed experimentally. In Table 8, the calculated frequencies and oscillator strengths of the $\Delta v_{CH} = 2-7$ overtones associated with the four methine groups of adamantane are given.

It is common to compare the relative intensities of different CH oscillators in a molecule; in this case it would be the

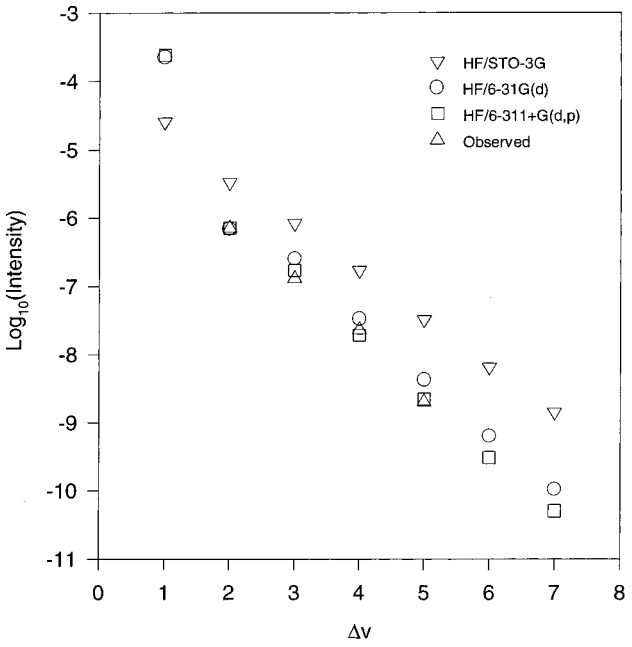

Figure 18. Observed and calculated total oscillator strengths of the CH stretching regions of adamantane. The observed intensities were obtained from solution-phase spectra.

methylene versus the methine. However, the methine and methlyene peaks were not well-resolved and the areas of the bands reported by Spectra Calc have a relatively high uncertainty. Thus only the total oscillator strengths, that is, $f_{tot} = f_{CH} + f_{CH_2}$, within a given vibrational manifold are compared with the observed values. The $\Delta v_{CH} = 2-5$ overtone spectra of adamantane in solution were used to calculate the observed oscillator strengths.

In Figure 18 the total observed oscillator strengths are compared to the calculated oscillator strengths obtained with the various basis sets. The intensities obtained with the 6-31G(d) and especially the 6-311+G(d,p) basis sets agree very well with the observed intensities. All of the calculated results successfully reproduce the observed decrease in intensity with increasing v. However, the STO-3G results overestimate the overtone intensities by approximately an order of magnitude, indicating that the dipole moment functions calculated with this basis set are not as good. In general the HF/6-311+G(d,p) basis set is more than adequate for the calculation of overtone intensities, as indicated in a study of H_2O.[40] The use of even larger basis sets usually gives results closer to experimental values,[40] but when a molecule the size of adamantane is considered, such calculations can be time consuming. The total CPU time of the HF/6-311+G(d,p) intensity calculation was approximately 30 days on a SGI model R4000 workstation with an IP20 processor. The application of an even larger basis set likely would not be worth the extra computer time, taking into account the excellent agreement obtained with the 6-311+G(d,p) basis set. In fact even the smaller HF/6-31G(d) calculation yields results that would be useful in spectral assignments. To our knowledge, this is the largest molecule for which overtone intensities have been calculated.

Conclusion

We have used conventional and photoacoustic laser spectroscopy to measure the overtone spectra of adamantane, 1-chloroadamantane, and hexamethylenetetramine in various phases and at several temperatures. The overtone spectra provided evidence of changes in the CH stretching potential due to phase effects, namely, an increase in harmonicity of the CH oscillators in the condensed phases of adamantane and 1-chloroadamantane. The increase in harmonicity is attributed to solvent matrix perturbation.

The vapor-phase overtone spectra also provided information about the different types of CH stretching oscillators of the adamantanes. The spectra of adamantane vapor and 1-chloroadamantane vapor yielded two and three peaks, respectively, in the $\Delta v_{CH} = 5$ region as predicted from the ab initio geometry optimizations. The overtone spectra can discriminate between CH bonds that have ab initio differences in bond length of a milliangstrom. Thus ab initio CH bond lengths can be helpful in the spectral assignment of CH stretching overtone spectra.

The overtone spectrum of adamantane in the low-temperature ordered phase in the regions corresponding to $\Delta v_{CH} = 3$-5 provided insight into the number of nonequivalent CH bonds. The $\Delta v_{CH} = 3$ region of the ordered phase of adamantane was the best resolved, and four peaks were observed corresponding to the four nonequivalent CH bonds. The $\Delta v_{CH} = 4$ and 5 regions were not as well resolved, but were significantly broader than the bands of the disordered phase. The broadening of the overtone peaks of the ordered phase of adamantane occurs due to the increase in the number of nonequivalent CH bonds and the resultant local mode splitting.

Adamantane overtone intensities and frequencies were calculated with the use of vibrational wave functions and eigenenergies from an anharmonic oscillator local mode model and a Taylor series expanded ab initio dipole moment function. The total oscillator strengths obtained with the dipole moment functions calculated with the HF/6-311+G(d,p) basis set were in excellent agreement with the observed values.

Acknowledgment. We are grateful to Professor Henrik Kjaergaard for helpful discussions and assistance and to Professor George Ferguson for his help with the X-ray crystal structures. Funding for this research has been provided by the Natural Sciences and Engineering Research Council of Canada.

References and Notes

(1) Hayward, R. J.; Henry, B. R. *J. Mol. Struct.* **1975**, *57*, 221.
(2) Henry, B. R. *Acc. Chem. Res.* **1977**, *10*, 207.
(3) Mortensen, O. S.; Henry, B. R.; Mohammadi, M. A. *J. Chem. Phys.* **1981**, *75*, 4800.
(4) Child, M. S.; Lawton, R. T. *Faraday Discuss. Chem. Soc.* **1981**, *71*, 273.
(5) Sage, M. L.; Jortner, J. *Adv. Chem. Phys.* **1981**, *47*, 293.
(6) Child, M. S. *Acc. Chem. Res.* **1985**, *18*, 45.
(7) Henry, B. R.; Swanton, D. J. *J. Mol. Struct. (THEOCHEM)* **1989**, *202*, 193.
(8) Mortensen, O. S.; Ahmed, M. K.; Henry, B. R.; Tarr, A. W. *J. Chem. Phys.* **1985**, *72*, 3903.
(9) Tarr, A. W.; Swanton, D. J.; Henry, B. R. *J. Chem. Phys.* **1986**, *85*, 3463.
(10) Kjaergaard, H. G.; Yu. H.; Schattka, B. J.; Henry, B. R.; Tarr, A. W. *J. Chem. Phys.* **1990**, *93*, 6239.
(11) Kjaergaard, H. G.; Henry, B. R. *J. Chem. Phys.* **1992**, *96*, 4841.
(12) Kjaergaard, H. G.; Turnbull, D. M.; Henry, B. R. *J. Chem. Phys.* **1993**, *99*, 9438.
(13) Turnbull, D. M.; Kjaergaard, H. G.; Henry, B. R. *Chem. Phys.* **1995**, *195*, 129.
(14) Kjaergaard, H. G.; Henry, B. R. *J. Phys. Chem.* **1995**, *99*, 899.
(15) Amoureux, J. P.; Bee, M.; Damien, J. C. *Acta Crystallogr. Sect. B* **1980**, *36*, 2633.
(16) Corn, R. M.; Shannon, V. L.; Snyder, R. G.; Strauss, H. L. *J. Chem. Phys.* **1984**, *81*, 5231.
(17) Jenkins, T. E.; Lewis, J. *Spectrochim. Acta Part A* **1980**, *36*, 259.
(18) Burns, G.; Dacol, F. H.; Welber, B. *Solid State Commun.* **1979**, *32*, 151.
(19) Wu, P. J.; Hsu, L.; Dows, D. A. *J. Chem. Phys.* **1971**, *54*, 2714.
(20) Henry, B. R.; Sowa, M. G. *Prog. Anal. Spectrosc.* **1989**, *12*, 349.

(21) Henry, B. R.; Kjaergaard, H. G.; Niefer, B.; Schattka, B. J.; Turnbull, D. M. *Can. J. Appl. Spectrosc.* **1993**, *38*, 42.

(22) Schattka, B. J.; Turnbull, D. M.; Kjaergaard, H. G.; Henry, B. R. *J. Phys. Chem.* **1995**, *99*, 6327.

(23) Kjaergaard, H. G.; Henry, B. R. *J. Phys. Chem.* **1996**, *100*, 4749.

(24) Spectra Calc is a commercially available product from Galactic Industries Corporation. Marquardt's nonlinear least-squares fitting algorithm is used: Marquardt, D. W. *J. Soc. Ind. Appl. Math.* **1963**, *11*, 431.

(25) Atkins, P. W. *Molecular Quantum Mechanics*, 2nd ed.; Oxford University: Oxford, 1983.

(26) Kjaergaard, H. G.; Proos, R. J.; Turnbull, D. M.; Henry, B. R. *J. Phys. Chem.* **1996**, *100*, 19273.

(27) *CRC Handbook of Chemistry and Physics*, 73rd ed.; Chemical Rubber: Boca Raton, FL, 1992.

(28) Kjaergaard, H. G.; Goddard, J. D.; Henry, B. R. *J. Chem. Phys.* **1991**, *95*, 5556.

(29) Kjaergaard, H. G.; Mortensen, O. S. *Chem. Phys.* **1989**, *138*, 237.

(30) Messiah, A. *Quantum Mechanics*; Wiley: New York, 1961.

(31) Wilson, E. B.; Decius, J. C.; Cross, P. C. *Molecular Vibrations*; McGraw Hill: New York, 1955.

(32) Frisch, M. J.; Trucks G. W.; Head-Gordon, M.; Gill, P. M. W.; Wong, M. W.; Foresman, J. B.; Johnson, B. G.; Schlegel, H. B.; Robb, M. A.; Replogle, E. S.; Gomperts, R.; Andres, J. L.; Raghavachari, K.; Binkley, J. S.; Gonzalez, C.; Martin, R. L.; Fox, D. J.; Defrees, D. J.; Baker, J.; Stewart, J. J. P.; Pople, J. A. *Gaussian 92*, Revision E.1; Gaussian Inc.: Pittsburgh, PA, 1992.

(33) Gray, C. G.; Gubbins, K. E. *Theory of Molecular Fluids*; Clarendon: Oxford, 1984; Vol. 1.

(34) Mecke, R.; Spiesecke, H. *Chem. Ber.* **1955**, *88*, 1997.

(35) Dellinger, B.; Kasha, M. *Chem. Phys. Lett.* **1976**, *38*, 9.

(36) Clark, T.; Knox, T. Mc. O.; Mackle, H.; McKervey, M. A. *J. Chem. Soc., Faraday Trans.* **1977**, *73*, 1224.

(37) Hassoon, S.; Snavely, D. L. *J. Chem. Phys.* **1993**, *99*, 2511.

(38) Niefer, B. I.; Kjaergaard, H. G.; Henry, B. R. *J. Chem. Phys.* **1993**, *99*, 5682.

(39) Broxton, T. J.; Deady, L. W.; Kendall, M.; Topson, R. T. *Appl. Spectrosc.* **1971**, *25*, 600.

(40) Kjaergaard, H. G.; Henry, B. R. *Mol. Phys.* **1994**, *83*, 1099.